XXI IMEKO World Congress "Measurement in Research and Industry"
August 30 – September 4, 2015, Prague, Czech Republic

TOMOGRAPHICAL APPROACH IN 3-D TEMEPEARTURE DISTRIBUTION MEASUREMENT BY DIGITAL HOLOGRAPHY

Pavel Psota [1,2], *Roman Doleček* [1,2], *Vít Lédl*[1], *Petr Vojtíšek* [1], *Tomáš Vít* [3] , *Ondřej Matoušek* [1]

[1] Regional Centre for Special Optics and Optoelectronic Systems (TOPTEC), Institute of Plasma Physics, Academy of Sciences of the Czech Republic, Praha, Czech Republic, psota@ipp.cas.cz
[2] NTI, Faculty of Mechatronics, Technical university of Liberec, Liberec, Czech Republic, pavel.psota@tul.cz
[3]KEZ, Faculty of Mechanical Engineering, Technical university of Liberec, Liberec, Czech Republic, tomas.vit@tul.cz

Abstract – A digital holographic method for 3-D measurement of temperature distribution is introduced in this paper. It is based on digital holographic tomography employing only one digital camera. The method is applied for measurement of steady naturally convective flow of fluid and as well as for fast dynamic flow in the form of pulsatile jets of fluid.

Keywords: digital holography, digital holographic interferometry, tomography, temperature measurement, pulsatile jets.

1. INTRODUCTION

Holographic interferometry (HI) is used in measurement of phase objects with great success for more than 40 years. Since its start many different applications have been developed and tested [1]. Recent developments in digital holographic interferometry (DHI) made this technique even more convenient and many experimental difficulties were mitigated. HI as an experimental technique occupies important place in field of heat and mass transfer [2-7] measurement. HI is an exceptionally powerful technique in terms of measurement of two-dimensional or circularly symmetrical temperature fields but in its standard configuration the technique cannot be applied for general temperature field's measurement [1]. The digital holographic tomography is very promising technique which could arise after the "digital age" arrival. Prior to this move very complicated arrangements had to be constructed in order to measure general temperature distribution by tomographic approach [8-10], which usually employed the recordings from different directions made through different holograms. On the other hand, digital holographic tomography can be realized with use of only one camera. In this paper we show the way how to measure steady or dynamically developing general temperature fields employing tomographic approach.

2. PRINCIPLE OF THE METHOD

2.1. Digital Holography

Digital holography consists of two steps: the recording of the digital hologram and its reconstruction. For recording, CCD or CMOS sensors are used to capture microinterference pattern (digital hologram) in which the information about the phase of the incoming waves is encoded. The hologram H is formed by a superposition of a reference wave U_r and an object wave U_o :

$$H \approx \left|U_o + U_r\right|^2 = \left|U_o\right|^2 + \left|U_r\right|^2 + U_o U_r^* + U_r U_o^* . \quad (1)$$

Coherence of the both waves is a necessary condition for proper interference. Lack of suitable coherent sources had been a major issue after the discovery of holography. Digitally recorded hologram is transferred to a computer as an array of numbers. The propagation of optical fields is completely described by diffraction theory, which allows numerical reconstruction of the image as an array of complex numbers representing the amplitude and phase of the optical field. In comparison with classical holography, in DHI the reconstruction process is done completely numerically **Error! Reference source not found.**.

Let the phase object (e.g. temperature field) be located at a distance *d* far from the sensor of a digital camera having a coordinates ξ, η . For digital reconstruction the recorded hologram $H(\xi,\eta)$ is multiplied with a numerical model of the reference wave $r(\xi,\eta)$. For a planar reference wave we can assign $r(\xi,\eta) = 1$. The complex field in the image plane *U* is calculated by the Sommerfeld formula which describes the diffraction of a light wave by the hologram grating in distance *d* from the hologram**Error! Reference source not found.**:

$$U(x,y) = \frac{1}{j\lambda}\iint H(\xi,\eta) r^*(\xi,\eta) \frac{\exp(jkr)}{r} d\xi d\eta , \quad (2)$$

where

$$r = \sqrt{d^2 + (\xi - x)^2 + (\eta - y)^2} . \quad (3)$$

Coordinates in the image plane are denoted as x, y. The Sommerfeld integral is usually solved either by the so called convolution approach or by Fresnel transform [1]. In convolution method the reconstruction formula (2) can be interpreted as a superposition integral:

$$U(x,y) = \\ = \iint H(\xi,\eta) r^*(\xi,\eta) g(x-\xi, y-\eta) d\xi d\eta \quad (4)$$

with the impulse response:

$$g(x,y) = \frac{1}{j\lambda} \frac{\exp(jk\sqrt{d^2+x^2+y^2})}{\sqrt{d^2+x^2+y^2}}. \quad (5)$$

With regards to the fact, that free space constitutes a linear and shift invariant system, the superposition integral can be regarded as a convolution solved by convolution theorem:

$$U(x,y) = \\ = \Im^{-1}\left\{\Im(H(\xi,\eta) r^*(\xi,\eta)) \Im(g(x,y))\right\} \quad (6)$$

The Fourier transform of *g(x,y)* can be calculated and expressed analytically as well. This saves one Fourier transform for reconstruction.

2.2. Digital holographic interferometry

In the digital HI (DHI) the principles are similar to classical HI except the reconstruction of the two waves is performed numerically. At least two digital holograms H_1, H_2 are captured. The first hologram corresponds to an initial (reference) state of a temperature field and the second hologram is captured when the temperature field has undergone the change. Two wave fields are reconstructed from the digital holograms as complex fields represented by formula:

$$U_1(n\Delta x, m\Delta y) = |U_1(n\Delta x, m\Delta y)| \times \\ \times \exp[\varphi_1(n\Delta x, m\Delta y)],$$

$$U_2(n\Delta x, m\Delta y) = |U_2(n\Delta x, m\Delta y)| \times \\ \times \exp[\varphi_2(n\Delta x, m\Delta y)], \quad (7)$$

respectively. When the wave fields are divided one by another e.g. U_1/U_2, their phases φ are subtracted, and it can be shown that for the phase difference $\Delta\varphi$ holds an expression:

$$\Delta\varphi = \arg\left(\frac{\mathrm{Im}\{U_1\}\mathrm{Re}\{U_2\} - \mathrm{Im}\{U_2\}\mathrm{Re}\{U_1\}}{\mathrm{Im}\{U_1\}\mathrm{Im}\{U_2\} + \mathrm{Re}\{U_1\}\mathrm{Re}\{U_1\}}\right). \quad (8)$$

The possibility of direct access to the phase difference information is one of the major advantages of DHI over the classical HI, where the phase difference has to be evaluated by interference pattern analysis.

2.3. Temperature distribution measurement

Once we obtained the phase difference the measurement of temperature field distribution can be performed. The temperature distribution measurement is one of the most important applications of HI or DHI in fundamental and industrial research due to its outstanding sensitivity to phase variation. Variation of temperature field induces also a variation of refractive index of the fluid. Let's assume the first hologram is recorded with refractive index n_1 and the second hologram with n_2. The formula

$$\Delta\varphi = \frac{2\pi}{\lambda} \oint_L [\Delta n - n_\infty] dl, \quad (9)$$

expresses the relation between refractive index variation $\Delta n = n_2 - n_1$ and interference phase.

In (9) *dl* is taken as the differential distance along the line *L*, n_∞ is refractive index of surrounding air. The solution of (9) depends on the type of refractive index field distribution. If general refractive index field $n(\xi, z)$ is considered we can write the function in polar coordinates *(t,Φ)* as following

$$n(\xi, z) = n(t\cos\Phi, t\sin\Phi). \quad (10)$$

The determination of general (non-symmetrical) fields requires the analysis of a large number of holographic interferograms captured in tomographic sense. In this case the line integral transform (11) is mathematically equivalent to Radon Transform:

$$g(s,\theta) = \iint \frac{2\pi}{\lambda} n(\xi, z) \delta(\xi\cos\theta + z\sin\theta - s) d\xi dz, \quad (11)$$

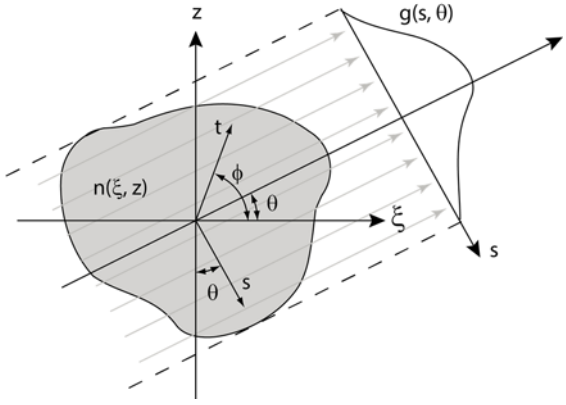

Fig. 1. The recording of asymmetric refractive index fields.

where *n(ξ,z)* is the refractive index distribution in Cartesian coordinates, δ is the Dirac pulse, θ is the angle of projection and *s* is the shift distance from the origin. For better understanding see Fig. 1. The projection data obtained by Radon Transform *g(s,θ)* is called sinogram. The name sinogram originated from the Radon transform of a Dirac delta function which is a distribution supported on the graph of a sine wave.

In practice, the sinogram is a 2D array containing the projections from different viewing directions in columns of the array. Reconstruction is based on back-projection mathematically described by Inverse Radon Transform:

$$n(\xi,z)=\frac{\lambda}{2\pi}\int_0^{\pi} g(\xi\cos\theta+z\sin\theta,\theta)d\theta\,. \quad (12)$$

The back-projection operation translates the measured sinogram back into the image space along the projection paths. Further, images for all rows are stacked to get 3D volume data.

The temperature field and refractive index field have relation given by the ideal gas equation and Gladston-Dale equation:

$$n-1=K.\rho\,. \quad (13)$$

In (13) K represents Gladston-Dale constant, which is property of gas. The Gladston-Dale constant is almost independent from pressure or temperature under the moderate physical conditions. It is slightly dependent on wavelength of the light. The density ρ of the gas is proportional to product of the pressure P and molecular weight M and inversely related to absolute temperature ϑ and $R=8{,}3143JK^{-1}mol^{-1}$ is the universal gas constant:

$$\rho=\frac{MP}{R\vartheta}\,. \quad (14)$$

Combining (13) with (14) yields to formula

$$n-1=\frac{KMP}{R\vartheta} \quad (15)$$

comprising the required temperature and the measured quantity - refractive index.

3. EXPERIMENT AND RESULTS

In order to get double sensitivity measurement setup the Twymann-Green based interferometer was proposed earlier [11, 12] . Working principle of such interferometer is shown in Fig. 2. The laser beam is divided by polarizing beam splitter BS_1. Further the beams are spatially filtered and collimated. Beam no. 1 is reflected by mirror M_2 to beam splitter BS_2. One part of the beam no. 1 goes directly through beamsplitter and objective O to digital detector. Second part is reflected to collimation objective CO and lost. Collimated beam no. 2 enters the beam splitter BS_2. One part of the beam no.2 is reflected in direction to M_2 and lost, second part passes through the measured object. Mirror M_3 is placed behind the object and it reflects the beam back through the object to the beam splitter BS_2. There the beam undergoes second division and part of it is directed through the objective O to the digital detector where the both beams are superposed.

This setup leads the beam to pass through the measured object twice which results in double sensitivity.

To demonstrate the reliability of the method we measured a temperature field of heated air flowing out from an orifice. The measurement was conducted in two different modes. Firstly, a steady naturally convective flow of fluid moving up from an orifice was measured and, secondly, the temperature field under investigation was stimulated by pulsatile jet of fluid with frequency of 15 Hz. Pulsatile jets (PJ) were generated by pushing/pulling fluid through the orifice. tomographic reconstruction, the system is rotated step by step at angle of 10° from 0° to 180°.

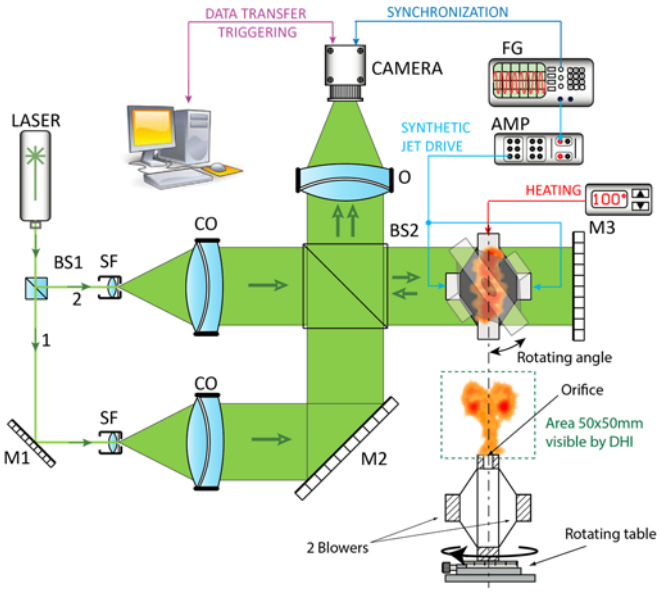

Fig. 2. Experimental holographic arrangements schematics of Michelson type of interferometer with double pass for tomographic measurement of PJs. BS1-polarizing beam splitter, SF-spatial filter, CO-collimation objective, BS2-nonpolarizing beamsplitter, O-objective lens, M-mirror.

The orifice has diameter 1 mm. The fluid (air) was heated in the cavity under the orifice in order to set temperature difference between the jet and surrounding fluid. The heating cartridge was heated to 100 °C, the temperature was controlled by PID regulator with maximum regulation error of 0.2°C. For tomographic processing we needed data from different projections, therefore we fixed the system on a 360° rotation platform stage. To achieve the

For measurement of steady temperature field the situation is quite straightforward. We captured a sequence of holograms as video sequence for all 18 equally spaced projections. All reconstructed phase fields from holograms corresponding to a certain projection were averaged in order to suppress random phenomena of flow. Holograms were reconstructed with use of formula (6). Before measurement we also captured, reconstructed and averaged phase fields of reference holograms with no mass flow.

The representation of the reconstructed phase data as a function of the angle is known as a sinogram. The 3-D temperature distribution can be reconstructed from the sinograms by a filtered backprojection algorithm as it was described in previous text. For this purpose, the standard inverse Radon transform (iradon) in MATLAB was used and implemented slice-by-slice along the rotation axis. Reconstructed temeperature distribution in 3D space is shown in Fig. 3.

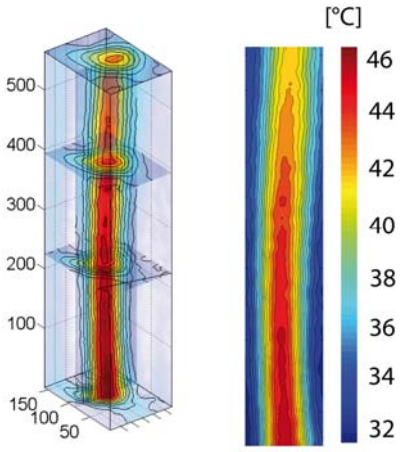

Fig. 3. Results of steady temperature field 3D (left) distribution measurement by DHI employing tomographical approach. One voxel in the left hand side plot represents space volume of 100 x 100 x 100 μm^3. False color image on the right hand side introduces temperature distribution along the central plane of the flow.

In case of PJ mode the temperature field is no longer steady and evinces dynamic character. Therefore, the camera capture time has to be synchronized and triggered in dependence of the PJ puff phase. The PJ is driven by function generator and the signal is amplified by amplifier. This setup enables to capture the digital hologram of the dynamic flow with a precisely defined delay (phase of the phenomenon). The coherence of the PJ phenomenon (self-similarity of repeated puff) is the key factor in enabling the meaningful triggering in order to capture holograms in the same relative phase of the phenomenon in every cycle, see Fig. 4.

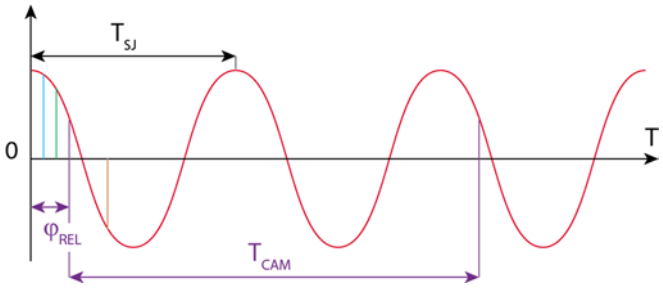

Fig. 4. Graphical display of synchronization and triggering between the phenomenon (red curve) and the camera. It enables to precisely capture user defined relative phase φ_{REL} of the phenomenon very precisely (note: T_{SJ} – period of pulsatile jets, φ_{REL} – relative phase of the phenomenon, T_{CAM} – capture time of the camera).

The cycle frequency in our experiment is higher than the maximum frame rate of the camera. The synchronization frequency is naturally higher than the camera frame rate, thus the stroboscopic type of approach must be applied. The hologram is not captured in every period when the trigger comes, but some cycles of the phenomenon are skipped between the captures. When the camera is ready and the trigger comes the frame is captured. Therefore it is possible to measure very high frequency coherent phenomena with use of a lower frame rate camera, . The coherence of PJs is also necessary for tomographic approach. Precise synchronization of the camera with the PJ driver can "freeze" the state of the phenomenon at a well-defined relative phase (time delay). At this firmly given relative phase a video sequence of holograms is captured. The same procedure is repeated step by step, when the table is rotated. The series of sequences consist of the sequences with the same time delays but the measurements are performed along different projection. This procedure is repeated unless the data for all projections are captured. The data processing in next steps does not differ from the above mentioned steady flow measurement.

Some results of PJ 3D temperature field measurement are displayed in Fig. 5. Measurements were conducted for three different phases of the phenomenon at relative times (from left) t/T=0.15, 0.30 and 0.45.

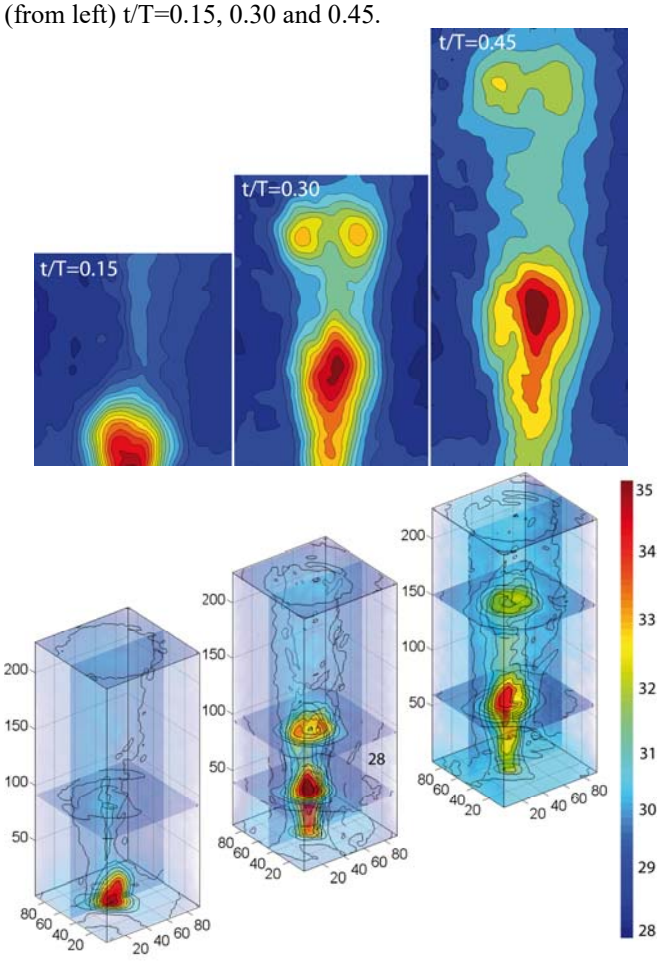

Fig. 5. Results of dynamic asymmetric temperature field distribution measurement (units are °C) by DHI employing tomographical approach. One voxel in the 3D plot (down) represents space volume of 100 x 100 x 100 μm^3. 2D false color images (up) introduce temperature distributions along the central plane of corresponding 3D plot at different relative times. Contour levels indicates temperature variation of 1°C.

4. DISCUSSION & CONCLUSIONS

The paper presents a simple and powerful digital holographic method for asymmetric temperature distribution measurement. Experimental arrangements is based on Twyman-Green holographic interferometer with double pass enhancing phase sensitivity by propagating the rays through the inspected area twice compared to more frequently used Mach-Zehnder interferometer. The 3D measurement is

based on tomographic approach and the data from different projections are captured and used for tomographic reconstruction.

Several sources of error which are influencing our measurement could be considered. The fundamental error source is the noise in measured phase fields of every projection. From the experimental data the maximum value of phase noise is estimated to be 0.025 rad. Considering our experimental arrangements such a phase noise introduces measurement error of temperature field (calculated for one projection) $\Delta\vartheta_{PN}$=0.98 °C. Source of error characteristic for tomography is hiden in calculation of inverse Radon transform. When visible light issued to probe fields above the millimeter range with weakly-varying refractive index the approximation of straight rays is obviously non-abusive [13]. This feature therefore can be neglected in our measurements. Gorski [14] analyzed quantitatively tomographic reconstructions of an optical fiber achieved under the straight rays hypothesis, compared his results with a simulation based on a Huyghens-Fresnel model taking diffraction into account, and confronted his results with experimental data. He demonstrated that even if a diffraction of light is considered the refractive index error is always about one order lower than the measured variation of refractive index. Heated air in our experiment generates variation of refractive index in order of 1E-6 and therefore the accuracy of inverse radon transform is in order of 1E-7. This fact brings error to our measurement $\Delta\vartheta_{IR}$=0.1°C. Combination of the inverse radon error $\Delta\vartheta_{IR}$ with the phase noise error $\Delta\vartheta_{PN}$ results in error $\Delta\vartheta=(\Delta\vartheta_{PN}^2+\Delta\vartheta_{IR}^2)^{0.5}\sim 1$ °C.

Obviously, the most significant source of errors is the phase development in time since the measurements along different projections are not performed simultaneously. Therefore we examined the variation of phase fields in time as a standard deviation for every pixel *(n,m)*:

$$\sigma(n,m)=\sqrt{1/N\sum_{i=1}^{N}\left(\Delta\varphi_i(n,m)-\overline{\Delta\varphi}(n,m)\right)^2}\ , \quad (16)$$

where $\overline{\Delta\varphi}(n,m)=1/N\sum_{i=1}^{N}\Delta\varphi_i(n,m)$ is the averaged phase field from N (in our experiment N=20) phase fields. For PJ measurement the maximal standard deviation in the area of active flow is 0.2 rad. This phase variation corresponds to temperature change of 8 °C which is not acceptable.

However, the nature of the PJ periodic flow can divide the instantaneous temperature flow $\vartheta(t)$ to parts $\overline{\vartheta},\vartheta_p(t/T),\vartheta_{rand}(t/T)$ representing the time-mean, periodic (coherent) and fluctuating (incoherent, random) components, respectively. The *t/T* indicates the phase during the cycle. This could be described by the equation

$$\vartheta(t)=\overline{\vartheta}+\vartheta_p(t/T)+\vartheta_{rand}(t/T)\,. \quad (17)$$

The time-mean component can be determined as: $\overline{\vartheta}=\lim_{T\to\infty}1/T\int_0^T\vartheta(t)dt$. For the periodic component holds: $\vartheta_p(t/T)=1/N\sum_{n=1}^{N}\vartheta(t+nT)$. It follows therefore that our method (employing the phase averaging) is sensitive only to the periodic part of the signal $\vartheta_p(t/T)$, for which the accuracy of our measurements approaches approximately the 1°C as derived earlier. Regarding minimal measured value of temperature 28°C and measurement error 1°C, the results are in range of 3.6% of measured value.

The same formulas and statements hold true for steady flows where the relative time *t/T* is simply replaced by instantaneous time *t* and the periodic component can be neglected. Averaging of phase fields suppresses the random part of the signal and therefore only time-mean temperature can be measured. Standard deviation of phase fields 0.1 radians (~4°C) in different times calculated by (16) gives us insight into random part of the temperature distribution. The time-mean temperature field is measured with the same error 1°C.

Moreover, to verify the reliability of our method, we compared results obtained by digital holographic tomography to results from well-established CTA (Constatnt Temperature Anemometry) [15-17]. CTA is a single point method and as a result the temperature values were measured only in few points. In the next step the results of CTA and DHI were compared. The both method are in a very good agreement falling into range of 10%. The holographic and CTA measurements were not performed simultaneously, which is probably the major source of data discrepancy.

ACKNOWLEDGMENTS

We gratefully acknowledge the support of the Grant Agency of the Czech Republic - Czech Science Foundation (project no. 14-08888S). The work of O. Matoušek and P.Psota was also supported by the Ministry of Education of the Czech Republic within the SGS project no. 21066/115 on the Technical University of Liberec.

REFERENCES

[1] T. Kreis, *Handbook of holographic interferometry: optical and digital methods. 2005*. Weinheim: Wiley-VCH. xii.

[2] P. R. N. Childs, J. R. Greenwood, and C. A. Long, “Review of temperature measurement,” *Review of scientific instruments*, vol. 71, no. 8, pp. 2959–2978, 2000.

[3] C. Shakher and A. K. Nirala, “Measurement of temperature using speckle shearing interferometry,” *Applied optics*, vol. 33, no. 11, pp. 2125–2127, 1994.

[4] S. Kampmann, A. Leipertz, K. Döbbeling, J. Haumann, and T. Sattelmayer, “Two-dimensional temperature measurements in a technical combustor with laser Rayleigh scattering,” *Applied optics*, vol. 32, no. 30, pp. 6167–6172, 1993.

[5] D. Wilkie and S. A. Fisher, “Measurement of temperature by Mach-Zehnder interferometry,” *Proc. Inst. Mech. Eng*, vol. 178, pp. 461–472, 1963.

[6] V. Lédl, T. Vít, R. Doleček, and P. Psota, “Digital holografic interferometry used for identification of 2D temperature field,” *EPJ Web of Conferences*, vol. 25, p. 02014, Apr. 2012.

[7] C. M. Vest, “Interferometry of strongly refracting axisymmetric phase objects,” *Applied optics*, vol. 14, no. 7, pp. 1601–1606, 1975.

[8] D. Wang and T. Zhuang, “The measurement of 3-D asymmetric temperature field by using real time laser interferometric tomography,” *Optics and lasers in engineering*, vol. 36, no. 3, pp. 289–297, 2001.

[9] J. M. Oprins, G. J. Heynderickx, and G. B. Marin, "Three-dimensional asymmetric flow and temperature fields in cracking furnaces," *Industrial & engineering chemistry research*, vol. 40, no. 23, pp. 5087–5094, 2001.

[10] M. Antoš, "New three-dimensional configuration of multidirectional phase tomograph," in *15th Czech-Polish-Slovak Conference on Wave and Quantum Aspects of Contemporary Optics*, 2007, p. 66090R–66090R.

[11] R. Doleček, V. Lédl, V. Kopecký, P. Psota, J. Václavík, T. Vít, "Prospects of digital holographic interferometry in heat transfer measurement",*Experimental Fluid Mechanics*, 25-27, 2009.

[12] L. O. Heflinger, R. F. Wuerker and R. E. Brooks. "Holographic Interferometry". J. Appl.Phys. 37(2): 642–649 (1966).

[13] W. Gorski. "Tomographic microinterferometry of optical fibers". Optical Engineering 45(12):125002 (2006).

[14] R. Doleček, P. Psota, V. Lédl, T. Vít, J. Václavík, and V. Kopecký, "*General temperature field measurement by digital holography"* Applied Optics Vol. 52, Iss. 1, pp. A319–A325, 2013.

[15] S. G. Mallinson, J. A. Reizes, G. Hong, and P. S. Westbury, "Analysis of hot-wire anemometry data obtained in a synthetic jet flow," *Experimental thermal and fluid science*, vol. 28, no. 4, pp. 265–272, 2004.

[16] J. Smits, A. E. Perry, and P. H. Hoffmann, "*The response to temperature fluctuations of a constant-current hot-wire anemometer*," Journal of Physics E: Scientific Instruments, vol. 11, no. 9, p. 909, 2001.

[17] R. Doleček, P. Psota, V. Lédl, T. Vít, P. Dančová, and V. Kopeckỳ, "Comparison of digital holographic interferometry and constant temperature anemometry for measurement of temperature field in fluid," *SPIE Optics+ Optoelectronics*, 95080P , 2015.